AIAA SciTech Forum
6-10 January 2025, Orlando, FL
AIAA SCITECH 2025 Forum

10.2514/6.2025-1294

Laser Thomson Scattering Measurements in Low Density Pulsed Argon Plasma

Victorien P. Blanchard[1], Junaid A. Qureshi[2],
Department of Mechanical Engineering, Colorado State University, Fort Collins, CO, 80523, USA

Naoji Yamamoto[3]
Department of Interdisciplinary Engineering Sciences, Kyushu University, Kasuga 816-8580, Japan

Azer P. Yalin[4]
Department of Mechanical Engineering, Colorado State University, Fort Collins, CO, 80523, USA

This paper presents temporally-resolved electron number density and temperature in a custom glow discharge in Argon at 1.2 Torr to study the feasibility of detecting low electron number density. A setup consisting of a compact frequency-doubled nanosecond Nd:YAG laser and two Volume Bragg Grating notch filters for attenuation of stray light in the collection optics is used. The lowest electron number density measured is 2.5±0.5 x10^{17} m^{-3}. These results indicate that laser Thomson scattering is a suitable diagnostic for measurement of electron properties in low-density plasmas.

I. Introduction

Electric propulsion (EP) represents transformative advancement within spacecraft propulsion, providing significant advantages over conventional chemical propulsion systems for various mission profiles, including long-distance space missions and satellite station keeping. EP utilizes electrical energy for generating thrust which makes it a sustainable and efficient option for the long duration of space missions [1,2]. The key advantage of EP is that it has a higher specific impulse (I_{sp}), therefore reducing the fuel need for a given mission. Over the last 25 years, the specific power generated onboard spacecraft has increased from 30 W/kg to 100 W/kg over the past 25 years, with further projections up to 200 W/kg, and the average specific impulse has increased to ~1000 seconds in the past decade [3,4]. These features have attracted space companies to use EP, specifically Hall Effect Thrusters (HET), as the basic propulsion system.

Hall Effect Thruster comprises different key components. The anode and the gas distributor introduce the propellant into the thruster, where it is then ionized. The magnetic core and coils generate a magnetic field that traps electrons emitted from the cathode, enhancing the ionization process. Our focus is on the hollow cathode, which is responsible for emitting a stream of electrons that is the source for ionizing the propellant while also neutralizing the beam leaving

[1]Postdoctoral Research Fellow, Department of Mechanical Engineering, Colorado State University, Fort Collins, CO, Member AIAA
[2]Ph.D. Student, Department of Mechanical Engineering, Colorado State University, Fort Collins, CO
[3]Department of Interdisciplinary Engineering Sciences, Kyushu University, Kasuga 816-8580
[4]Professor, Department of Mechanical Engineering, Colorado State University, Fort Collins, CO, Associate Fellow AIAA

the spacecraft (preventing the spacecraft from charging). The hollow cathode (HC) is a crucial element in the HET, tasked with generating electrons essential for ionizing the propellant gas and neutralizing the ion beam. Therefore, the stability and the efficiency of the HCs directly affect the overall performance of the HETs, which also influences the I_{sp}, thrust levels, and the longevity of the operations.

Characterizing HETs and HCs has been a very active area of research over the past decades. Researchers have used various diagnostic techniques to investigate the operational behavior and plasma properties [5–10]. Some of the widely used methods include the usage of Langmuir probes [11]. Besides, Optical Emission Spectroscopy (OES) is a widely used technique to infer various parameters, including electron temperature, density, and species composition [12]. Moreover, laser-induced fluorescence (LIF) provides detailed information on ion distributions and velocities by exciting the specific molecular or atomic transitions and observing the fluorescence [13]. Finally, Laser Thomson Scattering (LTS), unlike probes, is a non-intrusive diagnostic that allows for detailed spatial and temporal resolution of electron properties [10,14–16].

Previous studies have used complex setups, including the use of the optical cavity and triple-grating monochromator. Although effective, these approaches have introduced significant challenges in terms of complexity and implementation in practical applications [6,9,17]. Recently, the use Volume Bragg Grating notch filters has allowed for more compact setups [8,10,14–16,18–20]. In this study, we propose to use a compact setup using a frequency-doubled nanosecond Nd:YAG laser and two Volume Bragg Grating notch filters for attenuation of stray light, as proposed in [10]. The goal of this study is to demonstrate that the proposed setup is suitable to measure electron properties in low-density plasmas similar to those produced by hollow cathodes. This work will focus on the characterization of a custom glow discharge in Argon at 1.2 Torr.

II. Experimental setup and diagnostic

A. Low-density plasma setup

The low-density plasma study is this article is produced by a custom glow electric discharge in a plasma reactor filled with Argon at 1.2 Torr. The interelectrode gap is set to 4 mm and the voltage between the electrode is generated by a pulsating boost chopper circuit. To ignite the plasma, 10 voltage pulses are applied at 20 kHz, then to match the laser repetition frequency, this burst is repetitively operated at 20 Hz. A typical voltage trace of a burst is shown in Figure 1

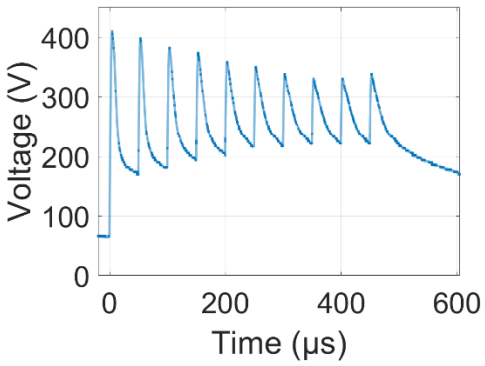

Figure 1. Typical voltage trace of the glow discharge in Argon at 1.2 Torr.

B. Laser Thomson scattering

Incoherent laser Thomson scattering results from the scattering of the laser light from unbound charged particles in the plasma [21]. Given the mass difference between ions and free-bound electrons, the contribution of ions to scattered light is negligible. The scattered light is proportional to the electron number density and electron temperature influences the scattering by introducing a Doppler shift. The total power scattered during the process is given by:

$$P_{Thomson} = \eta I_{laser} r_e^2 \Omega_s n_e V S(n_e, T_e, \lambda_0) \left(\hat{s} \times \left(\hat{s} \times \hat{E}\right)\right)^2 \quad (1)$$

Where η is the collection efficiency, I_{laser} the laser intensity, r_e the electron radius, Ω_s the collection solid angle, n_e the electron number density, V the probe volume, $S(n_e, T_e, \lambda_0)$ the Salpeter form factor, and $\left(\hat{s} \times \left(\hat{s} \times \hat{E}\right)\right)^2$ accounts for the signal dependence on the scattering and incident electric field vector orientation. To calibrate the Thomson spectra, rotational Raman spectra are collected in N_2 at known pressure and temperature.

The inherent challenges of Thomson scattering are the weakness of the signal and the very small frequency shift to the laser wavelength. Therefore, it is necessary to suppress the elastic scattered light from Argon atoms and background reflections in the system. In this study, two Volume Bragg Grating notch filters are used in the collection optics to achieve this goal.

The experimental setup is presented in Figure 2. A frequency-doubled pulsed Nd:YAG laser (Quantel Q-smart 100), with a pulse duration of 8 ns and an energy per pulse of 50 mJ is used at a repetition frequency of 20 Hz, synchronized with the pulsating boost chopper circuit which ignites the plasma. A prism is used to separate the 1064-nm light that remains after the second-harmonic generator. The beam is focused in the plasma chamber with a 500-mm plano-convex lens. The plasma chamber is equipped with Brewster windows and baffles to minimize reflections. Note that the last baffle in the delivery arm of the chambre is replaced by an iris to precisely adjust its opening. The scattered light is collected with a set of lenses and mirrors. An optical relay associated with a slit is used to form a spatial filter and prevent plasma emission to be collected. After the optical relay, a lens is used to ensure the collimation of light that is filtered by the VBG notch filters (OptiGrate BNF-532-OD4-11M and OptiGrate BNF-532-OD4-25), with a theoretical optical density of 4 at 532 nm and a bandwidth ≤ 0.3 nm. A periscope is used to rotate the image of the beam by 90° and align it with the slit of the spectrometer. Finally, the light is collected with a spectrometer (Acton Research SpectraPro 2300i, focal length: 0.3 m) equipped with a 1200 gr/mm grating blazed at 500 nm and an ICCD camera (Princeton Instruments model PM4-1024f-HB-FG-18-P43-CM). Given the low sensitivity of Thomson spectra to the instrumental broadening, the slit is opened to 130 µm to maximize the signal, which results in an instrumental broadening of 0.39 nm. All the collection optics are enclosed in a black box to prevent any light from entering the slit of the monochromator without passing through the VBGs. Spectra are acquired with gate exposure of 8 ns to account for the jitter of the laser, and are obtained from the averaging of 5 to 10 set of signals accumulated 5000 times on the CCD.

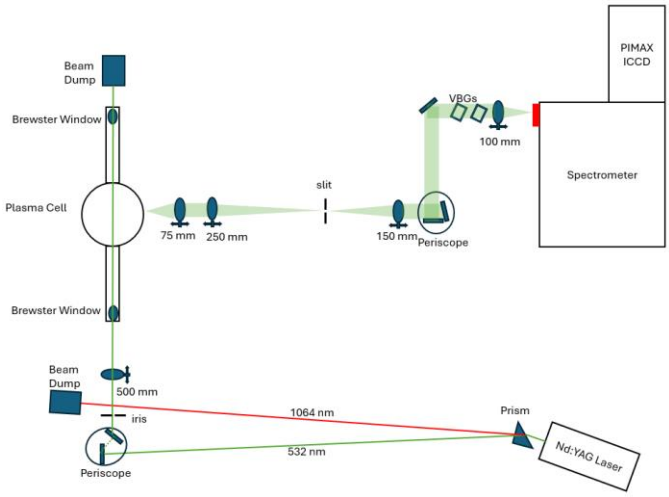

Figure 2. Schematic of the experimental setup, including the laser beam delivery, the plasma chamber, and the collection system.

The transmission curve of a VBGs is a function of the angle between the light and the VBG. Therefore, if we consider an object plane whose light is collimated when going through the VBG, only the light that falls within the angular range of rejection will be filter by the VBG. As explained by Bak *et al.* [16], the rejection zone defines a ring, whose width and radius depends on the focal length of the collimating lens and the angular filtering properties of the VBG. In practice, this means that the efficiency of the rejection rings depends on the magnification of the system and the quality of light collimation. An image of the beam and the rejection ring is shown in Figure 3. The position of the

rejection ring is adjusted with the pitch and yaw angle of the VBG. In our setup, the two rejection rings resulting from the two VBGs tangential to the image of beam and are overlapped with their curvature in opposite directions.

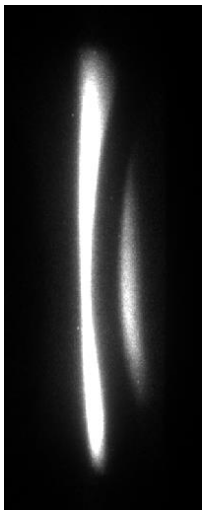

Figure 3. Image of the laser beam and the rejection ring captured with the ICCD camera and the grating of the spectrometer at 0th order.

Note that, the VBGs are reflective filters, which means that the light at 532 nm is reflected, and therefore, the alignment of the collection optics should be carefully done to avoid any of this reflected light to enter the spectrometer. Otherwise, this light could easily dominate the Thomson spectrum. A simple test consists of covering the last focusing lens in front of the slit of the spectrometer, and see if there is any residual light entering the spectrometer without being collected by the optics.

III. Results and discussion

Figure 4 shows a typical Thomson spectrum calibrated and fitted to infer the electron temperature and number density. The experimental spectrum is obtained from subtracting the signal with the laser OFF and the plasma ON to the signal with the plasma ON and the laser OFF, to ensure that the plasma emission is not included in the analysis. The suppression of the light at 532 nm by the VBGs is clearly visible in the experimental spectrum. The signal to noise ratio remains relatively high under these conditions because of the number of accumulations. Further increasing the signal would allow to optimize the acquisition parameters to improve it. Finally, Figure 4 shows that the fitting procedure has an uncertainty of ± 0.5 10^{17} m^{-3} and ± 0.2 eV.

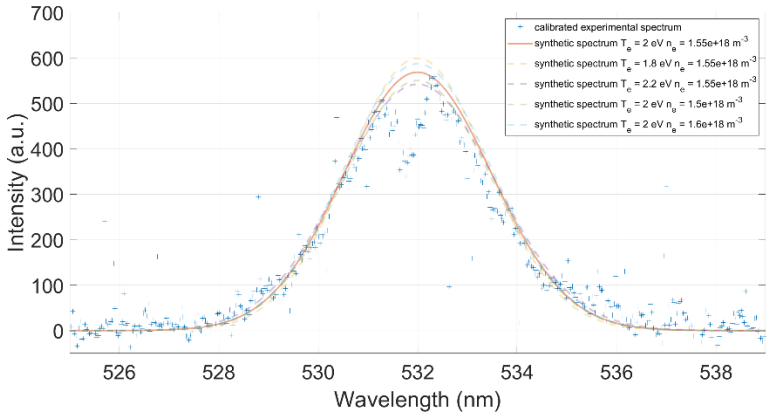

Figure 4. Typical fit of an experimental Thomson spectrum. The synthetic spectra with the solid line corresponds to the best fit and spectra with the dashed line are added to illustrate the uncertainty of the fit.

To investigate the detection of the current setup, we performed temporally resolved measurements of the third pulse shown in Figure 1. The results are shown in Figure 5. The electron number density is the highest when the voltage reaches its peak with a value of 9±0.5 $x10^{17}$ m^{-3}. Then, the electron number density slowly decays down to 2.5±0.5 $x10^{17}$ m^{-3} before the start of the following pulse. The electron temperature remains constant within the fit uncertainty at a value of 1.5±0.2 eV.

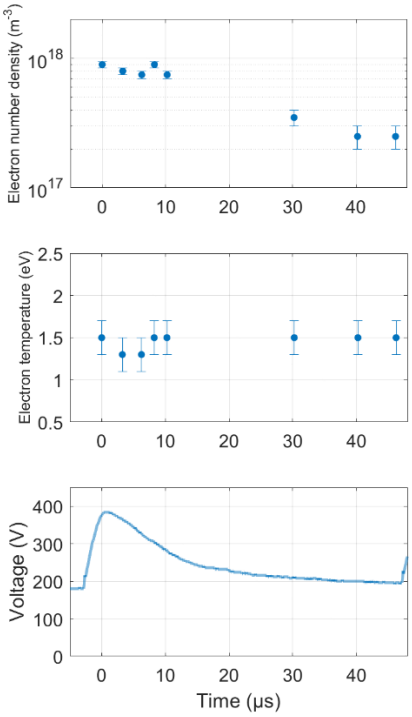

Figure 5. Temporal evolution of the electron number density, temperature, and voltage applied at the anode.

This study will employ a novel LTS-based diagnostic technique for characterizing HCs within HETs. Previous results in a similar HC setup showed that the electron number density and temperature are about $\sim 10^{18}\,m^{-3}$ and ~3 eV [9], which is in the range of the LTS technique with two VBG notch filters developed in [10].
This study will provide 2D electron number density and temperature maps, revealing detailed spatial variations. Enhanced sensitivity allows for a comprehensive understanding of electron emission properties under various operational conditions. Future work will focus on validating these results and further optimizing the technique, promising advancements in EP technology through more efficient and reliable cathode diagnostics.

IV. Conclusions

This study investigate the use of Volume Bragg Grating notch filters for laser Thomson scattering measurements. A custom glow discharge in Argon at 1.2 Torr is chosen as a test case for the diagnostic. The detection limit of the setup is found to be 2.5±0.5 $x10^{17}$ m^{-3}.
Previous results in the plume of barium oxide hollow cathode showed that the electron number density and temperature are about $\sim 10^{18}\,m^{-3}$ and ~3 eV [9]. Electron number densities down to $2x10^{17}$ m^{-3} were measured in the krypton plume of a lanthanum hexaboride hollow cathode [20]. The current work also reports a detection limit of $2x10^{17}$ m^{-3}. Therefore, future work will employ this diagnostic to measure 2D electron number density and temperature maps in the plume of a barium oxide hollow cathode.

Acknowledgments

We acknowledge financial support from the National Science Foundation Division of Physics under Award No. 2010466.

References

[1] Lev D, Myers RM, Lemmer KM, Kolbeck J, Koizumi H, Polzin K. The technological and commercial expansion of electric propulsion. Acta Astronautica 2019;159:213–27. https://doi.org/10.1016/j.actaastro.2019.03.058.

[2] Tajmar M. Chemical Propulsion Systems. Advanced Space Propulsion Systems, Vienna: Springer Vienna; 2003, p. 23–42. https://doi.org/10.1007/978-3-7091-0547-4_3.

[3] Jovel DR, Walker MLR, Herman D. Review of High-Power Electrostatic and Electrothermal Electric Propulsion. Journal of Propulsion and Power 2022;38:1051–81. https://doi.org/10.2514/1.B38594.

[4] Schonherr T, Komurasaki K, Romano F, Massuti-Ballester B, Herdrich G. Analysis of Atmosphere-Breathing Electric Propulsion. IEEE Transactions on Plasma Science 2015;43:287–94. https://doi.org/10.1109/TPS.2014.2364053.

[5] Biel W, Magd AA-E, Kempkens H, Uhlenbusch J. Study of oscillating magnetized hollow cathode arcs by time-resolved Thomson scattering measurements. Plasma Physics and Controlled Fusion 1995;37:599–610. https://doi.org/10.1088/0741-3335/37/6/001.

[6] Yamasaki K, Okuda K, Kono J, Saito A, Mori D, Suzuki R, et al. Development of the Thomson scattering measurement system for cascade arc device with indirectly heated hollow cathode. Journal of Instrumentation 2023;18:C11007. https://doi.org/10.1088/1748-0221/18/11/C11007.

[7] Jauernik P, Kempkens H, Uhlenbusch J. Simultaneous detection of Rayleigh and Thomson scattering signals from a hollow cathode arc plasma. Plasma Physics and Controlled Fusion 1987;29:1615–30. https://doi.org/10.1088/0741-3335/29/11/003.

[8] Roberts PJ, Jorns B. Characterization of Electron Mach Number in a Hollow Cathode with Thomson Scattering. AIAA SCITECH 2023 Forum, Reston, Virginia: American Institute of Aeronautics and Astronautics; 2023, p. 843. https://doi.org/10.2514/6.2023-0843.

[9] Friss AJ, Yalin AP. Cavity-enhanced Thomson scattering measurements of electron density and temperature in a hollow cathode discharge. Optics Letters 2018;43:5343. https://doi.org/10.1364/OL.43.005343.

[10] Yamamoto N, Yalin AP. Portable Thomson scattering system for temporally resolved plasma measurements under low density conditions. Review of Scientific Instruments 2024;95. https://doi.org/10.1063/5.0180534.

[11] Becatti G, Pedrini D, Kasoji B, Giusti N, Pieri L, Tellini C, et al. Plasma plume diagnostics of a LaB 6 hollow cathode with triple Langmuir probes. Journal of Instrumentation 2019;14:C08009–C08009. https://doi.org/10.1088/1748-0221/14/08/C08009.

[12] Lev DR, Alon G. Operation of a Hollow Cathode Neutralizer for Sub-100-W Hall and Ion Thrusters. IEEE Transactions on Plasma Science 2018;46:311–8. https://doi.org/10.1109/TPS.2017.2779409.

[13] Dodson C, Perez-Grande D, Jorns B, Goebel DM, Wirz RE. Laser-induced Fluorescence Measurements of Energetic Ions in a 100-A LaB6 Hollow Cathode Plume. 52nd AIAA/SAE/ASEE Joint Propulsion Conference, Reston, Virginia: American Institute of Aeronautics and Astronautics; 2016, p. 4838. https://doi.org/10.2514/6.2016-4838.

[14] Tsikata S, Hara K, Mazouffre S. Characterization of hollow cathode plasma turbulence using coherent Thomson scattering. Journal of Applied Physics 2021;130. https://doi.org/10.1063/5.0071650.

[15] Vincent B, Tsikata S, Mazouffre S, Minea T, Fils J. A compact new incoherent Thomson scattering diagnostic for low-temperature plasma studies. Plasma Sources Sci Technol 2018;27:055002. https://doi.org/10.1088/1361-6595/aabd13.

[16] Bak J, Suazo Betancourt JL, Rekhy A, Abbasszadehrad A, Miles RB, Limbach CM, et al. High resolution spatially extended 1D laser scattering diagnostics using volume Bragg grating notch filters. Review of Scientific Instruments 2023;94:023003. https://doi.org/10.1063/5.0121436.

[17] Koiso T, Yamashita Y, Tsukizaki R, Nishiyama K. Measurements of electron velocity distribution function in microwave cathode plume by incoherent laser Thomson scattering. Vacuum 2024;220:112760. https://doi.org/10.1016/j.vacuum.2023.112760.

[18] Vincent B, Tsikata S, Potrivitu G-C, Garrigues L, Sary G, Mazouffre S. Electron properties of an emissive cathode: analysis with incoherent thomson scattering, fluid simulations and Langmuir probe measurements. J Phys D: Appl Phys 2020;53:415202. https://doi.org/10.1088/1361-6463/ab9974.

[19] Roberts PJ, Jorns BA. Laser Measurement of Anomalous Electron Diffusion in a Crossed-Field Plasma. Phys Rev Lett 2024;132:135301. https://doi.org/10.1103/PhysRevLett.132.135301.

[20] Suazo Betancourt JL, Butler-Craig N, Lopez-Uricoechea J, Bak J, Lee D, Steinberg AM, et al. Thomson scattering measurements in the krypton plume of a lanthanum hexaboride hollow cathode in a large vacuum test facility. Journal of Applied Physics 2024;135:083302. https://doi.org/10.1063/5.0180251.

[21] Hutchinson IH. Principles of Plasma Diagnostics. 2nd ed. Cambridge University Press; 2002. https://doi.org/10.1017/CBO9780511613630.